Jul 5th, 12:00 AM - Jul 8th, 12:00 AM

Particle Image Velocimetry (PIV) Investigation of Local Scour Around Emergent and Submerged Circular Cylinders

P. Williams
University of Windsor, williamq@uwindsor.ca

R. Balachandar
University of Windsor

V. Roussinova
University of Windsor

R. Barron
University of Windsor

Particle Image Velocimetry (PIV) Investigation of Local Scour Around Emergent and Submerged Circular Cylinders

P. Williams[1], R. Balachandar[1], V. Roussinova[2] and R. Barron[3]
[1]Department of Civil and Environmental Engineering
University of Windsor
Windsor, ON N9B 3P4
CANADA
[2]Department of Mechanical, Automotive and Materials Engineering
University of Windsor
Windsor, ON N9B 3P4
CANADA
[3]Department of Mathematics and Statistics
University of Windsor
Windsor, ON N9B 3P4
CANADA
E-mail: williamq@uwindsor.ca

Abstract: *Analysis of the velocity field surrounding a circular cylinder under equilibrium of local scour has been restricted due to practical limitations of commonly used measurement techniques. This investigation summarizes select cases in the literature which have attempted to circumvent such limitations and presents flow field measurements using Particle Image Velocimetry (PIV). Scour tests were conducted in a horizontal flume fitted with a sediment recess containing erodible bed material. Tests were conducted with both emergent and submerged circular cylinders for a period of 24 hours, after which equilibrium was achieved and planar PIV measurements were obtained in the streamwise-vertical symmetry plane. Analysis of bed profiles and the distribution of the mean velocity indicated that the scour depth upstream of the cylinder was slightly (2 percent) higher for the emergent case, and separation of flow over the top of the submerged cylinder affected the formation of the dune in the wake of the cylinder.*

Keywords: *erosion, local scour, Particle Image Velocimetry (PIV), pier scour, scour modelling*

1. INTRODUCTION

Scour and erosion have been repeatedly established as the principal cause of most bridge failures in North America (Melville & Coleman, 2000, LeBeau & Wadia-Fascetti, 2007). The number of high-profile collapses spanning the past several decades are an indication of the need for improved methods of the design of foundation head with respect to local scour. While the evaluation of foundation head is predominantly achieved using empirical equations, such methods have proven inaccurate. Failure to achieve geometric similitude certainly contributes to such inaccuracy; however, it has also been determined that there are some aspects of the mechanisms that drive local scour which are not well understood. Prior work has been primarily concerned with exploring the relationship between various scour-governing parameters and the bed formation at an equilibrium condition. While this is reasonable from a design perspective, since the maximum scour depth in the vicinity of the pier is the quantity by which the foundation head is established, the examination of bed formations alone does not provide an accurate depiction of the flow field surrounding a pier under equilibrium of local scour (Williams et al., 2016).

In order to fully appreciate the mechanism of local scour and the parametric framework necessary for scour design, flow field measurements in the vicinity of the cylinder are required. Although the existence of large-scale turbulence structures (i.e., the downflow, horseshoe vortex, wake vortices) in the flow field surrounding a cylinder under equilibrium of local scour are well understood, the effect of changes in flow, sediment and cylinder characteristics on their size and strength require further consideration for design purposes. However, acquisition of such detailed flow measurements is not easily achieved. Point measurements using Acoustic Doppler Velocimetry (ADV) and Laser Doppler

Velocimetry (LDV) are time consuming, which significantly reduces the size of the region over which data can be reasonably acquired. Furthermore, the use of a downward-facing ADV probe eliminates the possibility of measurements within five centimetres of the free surface, which can amount to a significant portion of shallow flow. The use of techniques such as LDV and Particle Image Velocimetry (PIV) are also limited in scour modelling since the presence of solid features such as the pier and the bed formations reduce optical access to some areas of flow. Even so, PIV is considered preferable in order to acquire data over the cross-sectional area of flow required for the necessary analysis.

The use of planar PIV in scour experiments has been met with some difficulty, largely due to the practical need for a transparent surface through which image capture can occur. Planar capture is then realistically restricted to the *XZ* and *XY* planes. Here, *X* is the streamwise coordinate direction, *Y* is the vertical coordinate direction and *Z* is the spanwise coordinate direction. While measurements in the *XZ* plane would be possible with orientation of the laser sheet perpendicular to the flume sidewall and positioning of the camera lens in the downward vertical direction atop of the flume, the primary intention of the present experiments was to capture the flow field in the *XY* plane, in which velocity measurements using ADV are commonly presented for scour experiments. The unscoured bed material does impede image capture in the region below the original bed level in this plane; however, PIV measurements were captured in the entire flow field above this location.

Unger and Hager (2007) reported on the characteristics of the downflow and horseshoe vortex around a bridge pier. The authors assumed that the flow field around a half-cylinder placed against a transparent flume sidewall in erodible sediment would be representative of half of the flow field around a full cylinder. PIV measurements were captured in the *XY* plane for this set-up, and as such measurements within the scour hole were obtainable. Practically, however, this configuration describes abutment scour, and cannot really be viewed as intended by the authors. Kirkil et al. (2008) were able to capture streamline patterns at the free surface in the wake region of flow around a circular cylinder with scour using a large-scale Particle Image Velocimetry (LSPIV) system in the *XZ* plane. Zhang et al. (2009) explored local scour around a spur dyke placed against a transparent flume sidewall in a sediment recess. PIV measurements were made in the *XY* and *XZ* planes, and due to the location of the spur dyke, flow field measurements were once again captured within the scour hole. Guan et al. (2019) used an oblique shooting method to capture PIV measurements within the scour hole upstream of a circular cylinder. In this method, the camera was tilted at an angle and the PIV data was corrected in post-processing to account for the angle. However, in using this method, the measurements are limited to a single field-of-view in the oblique plane. Furthermore, while it was reported that there was no ‘significant’ discrepancy between measurements acquired using the oblique shooting method and a normal shooting method, there are additional potential uncertainties that could arise in using such a method. In general, the limitations of PIV use in scour experiments are well-demonstrated in the literature.

In literature, the majority of scour investigations have been carried out for emergent cylinders. However, there are many practical examples of flow past submerged cylinders in the field, including well foundations of bridge piers, piers which are submerged during flooding, structures in floodplains during flood events, structures submerged in offshore or coastal tides or currents (Dey et al., 2008), such as sub-sea caissons, platform foundations and submerged cylindrical breakwaters (Zhao et al., 2010), and submerged vegetation in natural streambeds (Dey et al., 2008). Therefore, both emergent- and submerged-type cylinders have been considered in the present investigation.

2. METHODOLOGY

2.1. Description of the laboratory facility

The experimental investigation was carried out at the Ed Lumley Centre for Engineering Innovation at the University of Windsor in Windsor, Canada. The laboratory facility contains a horizontal flume that is 10.5 m long, 0.84 m deep and 1.22 m wide. A schematic of the flume is shown in Figure 1. The flume is fitted with two flow conditioners upstream of the test section, the first of which is constructed out of 0.5-in PVC pipe sections. The second flow conditioner consists of fine polycarbonate honeycomb sections. As shown in Figure 1, a PVC ramp leads to a sediment recess of 3.68 m in

length and 0.23 m in depth, encompassing the width of the flume. This test section is filled with granular material with median sediment diameter d_{50} = 0.74 mm, standard deviation of particle size σ_g = 1.34, coefficient of uniformity C_u = 1.6 and coefficient of gradation C_c = 0.96. The specific gravity of sediment was 2.65. The critical velocity of sediment (U_c) for the bed material was evaluated using standard methods, which are detailed in other works (Williams et al., 2016, 2018).

A boundary layer trip is located at the beginning of the sediment recess and the flow depth was adjusted by a gate at the downstream end of the flume. The flow is serviced by a 60-HP centrifugal pump. The flow was calibrated with v-notch weirs, using methods described in the U.S. Department of the Interior Bureau of Reclamation Water Measurement Manual (2001). The Kindsvater-Shen relationship and the 8/15 triangular weir equation were used to calculate the flow rate and develop the performance curve for the flume pump prior to installation of the test section. The orientation of the flume and experimental measurements correspond to *X* in the streamwise direction, *Y* in the vertical direction, and *Z* in the spanwise or transverse direction. The bed level was taken as zero in the *Y* direction for all experiments and the geometric centre of the cylinder was taken as the origin in the *XZ* plane. The mean velocity components *U* and *V* correspond to the velocity in the *X*- and *Y*-directions, respectively.

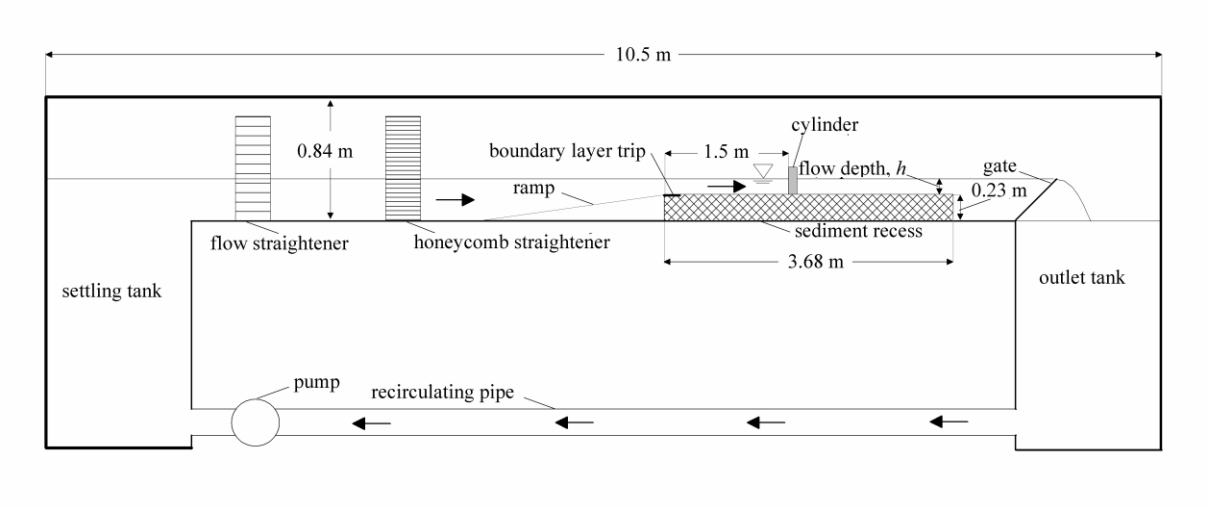

Figure 1 - Schematic of laboratory flume including test section details

2.2. Experimental program and test methodology

Prior to experimentation, PIV measurements were undertaken in the flow over the sand bed in the absence of a cylinder, in order to characterize the approach flow conditions. The depth-averaged velocity of the flow for all tests was determined to be *U* = 0.262 m/s. The flowrate *Q* for all experiments was 0.036 m^3/s. The cylinder diameter *D* for both tests was 0.056 m. The height of the submerged cylinder for test S1 was 1.88*D*. The width of the channel was adjusted using movable sidewalls to an effective width *b* = 0.40 m, corresponding to a blockage ratio *D*/*b* = 0.14. The depth of flow was held at *h* = 0.12 m for both tests in order to achieve a flow shallowness *h*/*D* of 2.14 such that the piers were classified as narrow.

Prior to testing, the sediment in the test section was carefully levelled using a trowel. For both cases, the necessary cylinder was installed in the centre of the channel. The flume was then filled with water to the desired depth. A calibration target for PIV image processing was suspended in the flume and calibration images were captured for each field-of-view. After the required calibration images were acquired, the target was removed from the flume and the pump was powered on and brought up to the required flow rate corresponding to a flow intensity (U/U_c) of approximately 0.85, to maintain clear-water conditions for local scour. The flow at the location of the cylinder was fully turbulent with a Reynolds number of 3.3×10^4 and subcritical with a Froude number of 0.26.

The tests were left to run for 24 hours before PIV measurements were taken. Prior analysis indicated

that equilibrium of scour was reached within 24 hours, and changes in the relative scour depth d_{se}/D were minimal beyond this point in time (D'Alessandro, 2013, Williams et al., 2019). PIV measurements were then undertaken for each required field-of-view (FOV). Prior to PIV measurements, the flow was seeded with 11-µm spherical glass particles. For each scour test, four fields-of-view were taken in the streamwise-vertical symmetry plane to ensure that the flow field was captured from the upstream extent of the scour hole to the end of the primary deposit in the wake region. A thin glass plate was suspended on the free surface in the region of interest during image capture to eliminate the distortion of the laser sheet from perturbations in the free-surface region.

After the required PIV images had been acquired, the pump frequency was gradually reduced in order to avoid disturbance of the bed sediment before the pump was powered off. The flume was then drained slowly to avoid disturbance of the scour formation and a Leica laser distance meter was used to measure the bed profile in the streamwise direction along the channel centreline (Z/D = 0). The uncertainty of the acquired bed measurements due to the accuracy of the laser distance meter was determined to be ±0.05 mm from the resolution of the point measurements.

2.3. Description of the PIV setup and data acquisition

A schematic of the two-dimensional planar Particle Image Velocimetry (PIV) system is shown in Figure 2. The PIV system was supplied by TSI and is comprised of several components, including an 8 MP Illunis CCD array camera and a dual pulse Litron Nd:YAG laser generating at 532 nm wavelength with an output energy of 135 mJ/pulse and a maximum repetition rate of 15 Hz. The laser sheet was expanded through a −15-mm cylindrical lens. The 8 MP camera was used to capture images with a resolution of 3312 × 2488 pixels in dual-capture mode. The camera was fitted with a 28-105 mm Nikkor lens. The laser was mounted on a mechanical traverse system affixed to a carriage on top of the flume, and such that the laser sheet could be moved in the streamwise direction as required. The camera was mounted on a tripod slider on the flume catwalk, aligned parallel to the flume sidewall and therefore the plane of symmetry. A TSI PIV LaserPulse synchronizer was used to synchronize image capture for the specified exposure time at the corresponding maximum pulse repetition rate (i.e., the time required for exposure and readout of two images) with the timing of the laser pulses for each frame (a single pair of images).

The test section for PIV measurements in the sediment recess was located at a streamwise distance of 1.5 m downstream of the boundary layer trip. Measurements were obtained in the XY or vertical plane. Through prior experimentation, it was established that between 2000 and 3000 frames captured at a rate of 2 Hz were adequate for time-averaged data acquisition. The optimal pulse separation (Δt, or the time step between two concurrent laser pulses) in the sequence was evaluated for each FOV by adjusting the value of the time step such that the average length of the post-processed vectors (i.e., the displacement of particles) in the region of interest was approximately 8 pixels. The total propagated uncertainty of the velocity measurements acquired by the PIV system was estimated to be ±0.015 m/s. The uncertainty analysis was based on the methods described in Park et al. (2008), which were adapted from the Visualization Society of Japan's (2002) guidelines.

PIV measurements for individual fields-of-view were taken and stitched together for each test. Slight discontinuities and scatter in the distribution of the velocities can be attributed in part to the variability in intensity along the laser sheet in the streamwise direction as well as reflections from the laser sheet on the bed and cylinder. There is also a strong out-of-plane component in the three-dimensional flow around a cylinder which is not captured by a planar PIV and the evaluation of Δt in such areas of cross-stream flow becomes complicated. Furthermore, the flow area within the scour hole was not captured due to the physical obstruction by the sediment recess in the field-of-view of the camera. Measurements in the region very close to the free surface were also not obtainable due to the presence of the glass plate in this region.

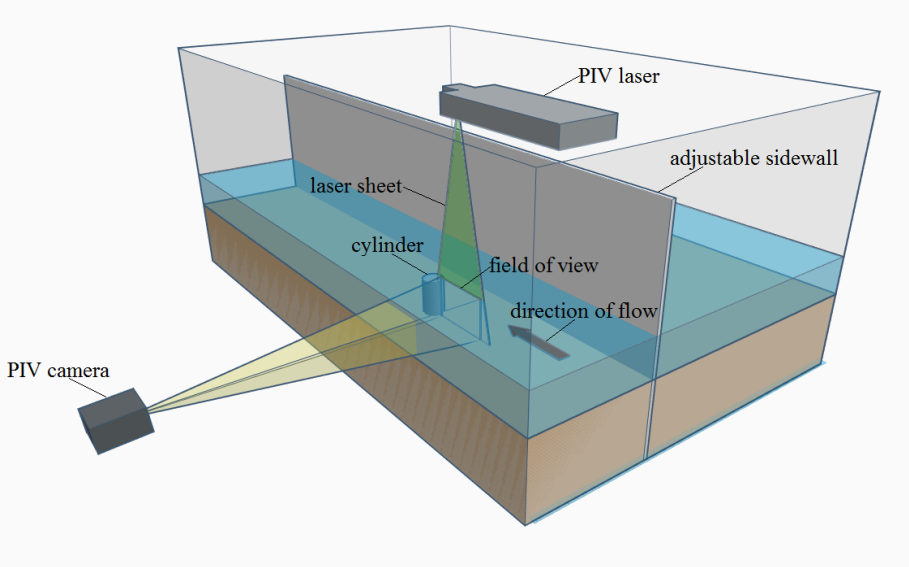

Figure 2 - Depiction of the Particle Image Velocimetry (PIV) system setup for image capture

2.4. PIV processing details

Post-processing of the PIV images was done using PIVlab, a GUI-based open-source MATLAB code (Thielicke & Stamhuis, 2019). PIVlab uses cross-correlation to determine displacement of illuminated tracer particles in the flow field. In PIVlab, a cross-correlation algorithm is used to determine vectors in the flow field by deriving the particle displacement between pairs of captured images. In this method, a "statistical pattern matching technique" is used to correlate the pattern of illuminated particles from a small interrogation area in each image of a pair, yielding a correlation matrix. The discrete cross correlation function is described by Eq. (1):

$$C(m,n) = \sum_i \sum_j A(i, j)\, B(i-m, j-n) \quad (1)$$

In Eq. (1), *A* corresponds to the interrogation area in the first image of a frame and *B* similarly corresponds to the interrogation area from the second image in the same frame. The cross-correlation technique attempts to "locate" the seeding pattern in *A* in a region with the same pattern in *B*, and the intensity peak in the generated correlation matrix *C* (based on the cross-correlation function) is deemed the "most probable" particle displacement between the interrogation areas in each image. (Thielicke & Stamhuis, 2014).

3. RESULTS AND DISCUSSION

Figure 3 shows the bed profile measurements for test E1 (emergent cylinder) and test S1 (submerged cylinder) in the *XY* symmetry plane at $Z/D = 0$ at an equilibrium condition, as well as a plan-view photograph of the scour formation for test S1. The profiles show that both cases result in a typical scour profile, with an inverted conical scour hole surrounding the cylinder and a dune-like primary deposit in the wake region. Upstream of the cylinder, Figure 3 shows that the scour depth is not significantly altered by the cylinder height. The scour profiles between tests E1 and S1 are very similar for $X/D < -0.5$. The depth of the scour hole is 2 percent deeper for test E1, which is reasonable since the downflow along the upstream face of the cylinder would be slightly stronger compared with the submerged case due to the increased projected area of the cylinder. In the wake region close to the cylinder ($0.5 < X/D < 3.0$), the scour depth for test S1 is very similar to that of test E1. Downstream of this point, from the leading edge of the dune onwards, the height of the scour formation is greater for test E1 and the length of the dune is greater for test E2. It appears that the dune dimensions are most affected by cylinder height.

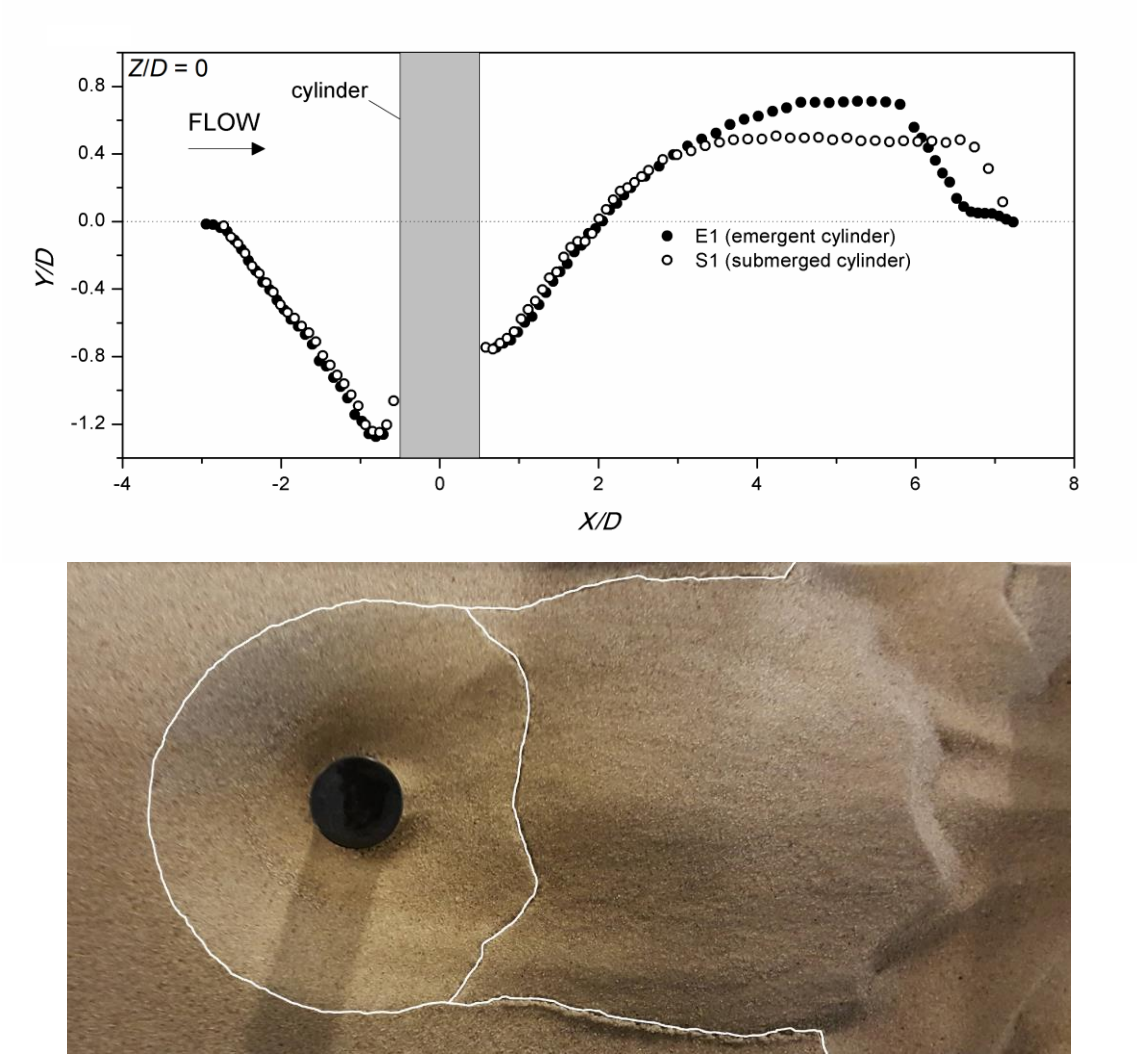

Figure 3 - Bed profile measurements for tests E1 and S1 in the XY symmetry plane at *Z*/*D* = 0 (top) and photograph of the scour formation for test S1 (bottom)

In Figure 4, the distribution of the mean streamwise velocity normalised by the maximum velocity of the undisturbed approach flow, U/U_e, is provided in the *XY* symmetry plane at *Z*/*D* = 0 for (a) test E1 and (b) test S1. The two-dimensional vector fields in the *XY* plane are also provided for (c) test E1 and (d) test S1. From the contours of U/U_e, certain features can be noted in the flow field for both tests. The adverse pressure gradient associated with the deceleration of the flow in advance of the upstream face of the cylinder is marked as feature 'A' for both tests. Feature 'C,' a region of low and negative mean streamwise velocity, is located in the immediate wake of the cylinder over the downstream portion of the scour hole. At the location of feature C, the vector fields for both tests E1 and S1 are also indicative of an upwash of flow emanating from the scour hole downstream of the cylinder. Further downstream, the acceleration of the flow up and over the primary deposit is noted as feature 'D,' and the separation of the flow from the crest of the dune is marked as feature 'E.' Each of these features is observed from the streamwise velocity contours as well as the vector fields.

A notable feature which is present in the flow field for the submerged case but not the emergent case is marked as feature 'B.' Feature 'B' is a region of flow separation emanating from the top of the submerged cylinder, characterized by an increase in the mean streamwise velocity. Although this region is located close to the free surface, it has affected the scour formation and the flow field since the flow in the submerged case is shallow. This increase in streamwise velocity near the cylinder's surface has caused an increase in erosion at the top of the primary deposit, reducing its height and increasing its length. It can also be noted that the magnitude of feature 'D' is higher in the region close to the cylinder for test S1 when compared with test E1, which is also likely to be attributable to the separation of flow and subsequent increase in *U* at the same downstream region.

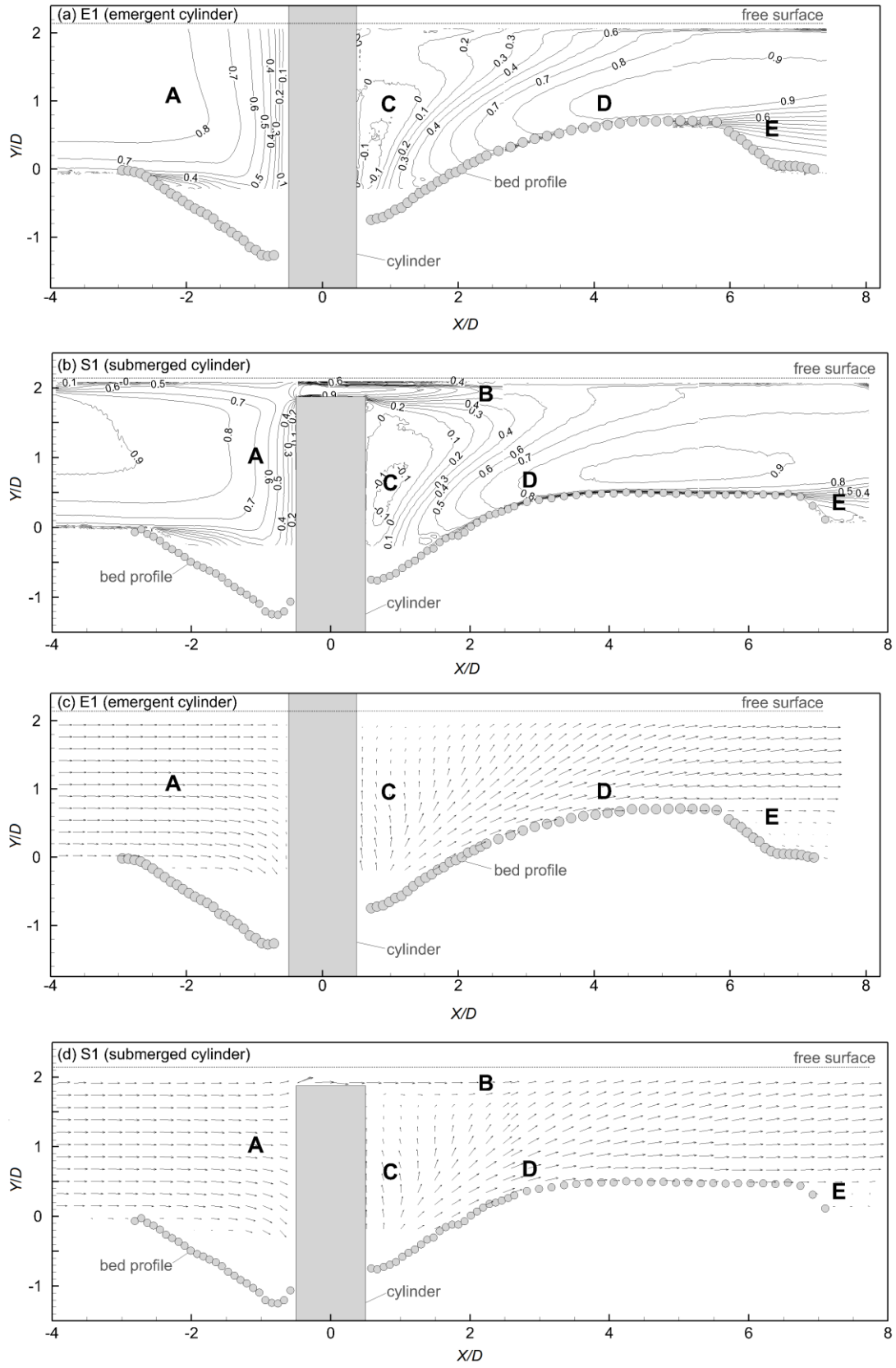

Figure 4 - (a) Distribution of U/U_e in the *XY* symmetry plane for test E1, (b) distribution of U/U_e in the *XY* symmetry plane for test S1, (c) two-dimensional vector field in the *XY* symmetry plane for test E1 and (d) two-dimensional vector field in the *XY* symmetry plane for test S1

4. CONCLUSIONS

The current investigation presents the methodology employed to acquire Particle Image Velocimetry (PIV) measurements for flume experiments involving equilibrium of local scour around circular cylinders. The results of two local scour experiments exploring the effects of cylinder height are presented. The bed profiles at equilibrium indicate that the depth of scour in the vicinity of the cylinder is not significantly affected by the cylinder submergence, but the width and length of the scour hole are greater for the emergent case. In the downstream region of the scour formation, the height and length of the dune are shown to be affected by cylinder height as well. The distribution of the mean streamwise velocity and the vector field in the streamwise vertical plane are shown to be very similar, with a region of high streamwise velocity due to the separation of the flow at the top of the cylinder visible for the submerged case and not the emergent case. This feature is shown to be responsible for the changes in the height and length of the primary deposit. In future experimental work, three-dimensional PIV measurements would be helpful in further exploration of the flow field surrounding a cylinder under equilibrium of local scour. Furthermore, although the two-dimensional PIV measurements do provide useful insight into the mechanism of local scour under varying geometry, there is a significant out-of-plane component of flow which should be captured in order to acquire a complete understanding of the flow field.

REFERENCES

D'Alessandro, C. (2013), *Effect of blockage on cylindrical bridge pier local scour* (Master's thesis). University of Windsor, Windsor, Canada.

Dey, S., Raikar, R.V., and Roy, A. (2008), *Scour at submerged cylindrical obstacles under steady flow.* J. Hydraul. Eng., 134(1), 105–109.

Guan, D., Chiew, Y.-M., Wei, M., and Hsieh, S.-C. (2019), *Characterization of horseshoe vortex in a developing scour hole at a cylindrical bridge pier*. Int. J. Sediment Res., 34(2), 118–124

Kirkil G., Constantinescu S. G., and Ettema R. (2008), *Coherent structures in the flow field around a circular cylinder with scour hole*. J. Hydraul. Eng., 134(5), 572–587.

LeBeau K. H., and Wadia-Fascetti S. J. (2007), *Fault tree analysis of Schoharie Creek bridge collapse*. J. Perform. Constr. Fac., 21(4), 320–326.

Melville, B. W., and Coleman, S. E. (2000), *Bridge Scour*. Water Resources Publication.

Park, J., Derrandji-Aouat, A., Wu, B., Nishio, S., and Jacquin, E. (2008), *Uncertainty analysis: Particle imaging velocimetry. ITTC Recommended Procedures and Guidelines*, International Towing Tank Conference (ITTC), Fukuoka, Japan, Sept, pp. 14–20.

United States Department of the Interior Bureau of Reclamation (2001), *Water Measurement Manual*. US Government Printing Office Washington, DC.

Thielicke, W., and Stamhuis, E. (2014), *PIVlab – Towards user-friendly, affordable and accurate digital particle image velocimetry in MATLAB*. J. Open Res. Softw., 2(1), e30.

Thielicke, W., and Stamhuis, E. J. (2019, September 6), PIVlab—Time-resolved digital particle image velocimetry tool for MATLAB.

Unger, J., and Hager, W. H. (2007), *Down-flow and horseshoe vortex characteristics of sediment embedded bridge piers*. Exp. Fluids, 42(1), 1–19.

Visualization Society of Japan. (2002), *Handbook of Particle Image Velocimetry*. Morikita Publishing Co. Ltd. (in Japanese).

Williams, P., Balachandar, R. and Bolisetti, T. (2019), *Examination of blockage effects on the progression of local scour around a circular cylinder*. Water, 11(12), 2631.

Williams, P., Bolisetti, T., and Balachandar, R. (2016), *Evaluation of governing parameters on pier scour geometry*. Can. J. Civ. Eng., 44(1), 48–58.

Williams, P., Bolisetti, T., and Balachandar, R. (2018), *Blockage correction for pier scour experiments*. Can. J. Civ. Eng., 45(5), 413–417.

Zhang, H., Nakagawa, H., Kawaike, K., and Baba, Y. (2009), *Experiment and simulation of turbulent flow in local scour around a spur dyke*. Int. J. Sediment Res., 24(1), 33–45.

Zhao, M., Cheng, L., & Zang, Z. (2010), *Experimental and numerical investigation of local scour around a submerged vertical circular cylinder in steady currents*. Coast. Eng., 57(8), 709–721.